

# Probe and Skip: Self-Predictive Token Skipping for Efficient Long-Context LLM Inference

Zimeng Wu<sup>\*1,2</sup> Donghao Wang<sup>\*1,2</sup> Chaozhe Jin<sup>1,2</sup> Jiaxin Chen<sup>1,2†</sup> Yunhong Wang<sup>1,2</sup>

## Abstract

Long-context inference enhances the reasoning capability of Large Language Models (LLMs), but incurs significant computational overhead. Token-oriented methods, such as pruning and skipping, have shown great promise in reducing inference latency, yet still suffer from inherently insufficient structure optimization, outdated selection criteria, and redundancy interference, resulting in suboptimal speed-accuracy trade-off. To address these issues, we propose a novel training-free framework dubbed Self-Predictive Token Skipping (SPTS), for efficient long-context LLM inference. Specifically, motivated by *probing the influence of target layers prior to skipping*, we design two selective token skipping strategies for typical structures, including Partial Attention Probing (PAP) for multi-head attention and Low-rank Transformation Probing (LTP) for feed forward network. The former selects informative tokens via partial forward attention computation, while the latter constructs a low-rank proxy network to predict token transformations. In addition, a Multi-Stage Delayed Pruning (MSDP) strategy reallocates skipping budgets and progressively removes redundant tokens across layers. Extensive experiments display the effectiveness of our method, achieving up to  $2.46\times$  and  $2.29\times$  speedups for prefilling and end-to-end generation, respectively, while maintaining state-of-the-art accuracy. We will release the source code upon acceptance.

## 1. Introduction

Recent advances in Large Language Models (LLMs) have significantly improved their capabilities in reasoning over long contexts (Liu et al., 2025a; Wang et al., 2024), en-

<sup>\*</sup>Equal contribution <sup>†</sup>Corresponding author <sup>1</sup>School of Computer Science and Engineering, Beihang University, Beijing, China <sup>2</sup>State Key Laboratory of Virtual Reality Technology and Systems, Beihang University, Beijing, China.

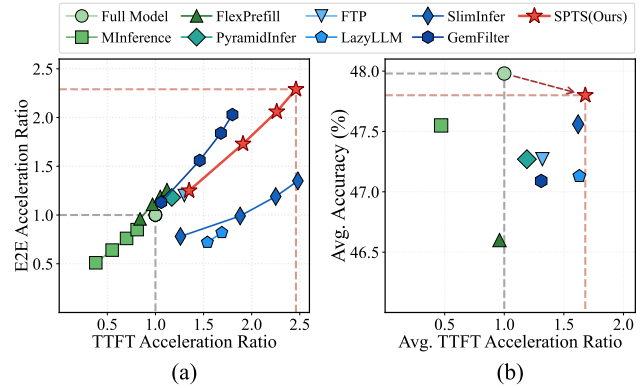


Figure 1. Efficiency-accuracy comparison on LLaMA-3.1-8B-Instruct (Dubey et al., 2024). (a) SPTS accelerates both prefilling and decoding, and achieves consistent speedups in first token (TTFT) and end-to-end (E2E) generation. (b) SPTS maintains higher accuracy at a more aggressive TTFT speedup ratios, with metrics averaged over the LongBench (Bai et al., 2024) dataset.

abling a wide range of applications such as multi-document question answering (Yang et al., 2018), few-shot learning (Zhong et al., 2021), and code completion (Liu et al., 2024). However, as the input sequence length increases, the computational overhead grows sharply, limiting the inference speed in both the prefilling and decoding phases under the standard auto-regressive paradigm (Liu et al., 2025a).

In order to reduce inference latency, a variety of acceleration strategies have been explored (Ma et al., 2023; Yang et al., 2024; Lai et al., 2025). Token pruning provides an effective solution by directly removing redundant tokens (Yang et al., 2024), but it incurs an inflexible trade-off between end-to-end acceleration and preservation of critical token information (Xu et al., 2025). Typically, the time cost of recomputing the pruned tokens always outweighs the speed gains from aggressive compression (Fu et al., 2024; Long et al., 2025). In contrast, sparse attention (Lai et al., 2025) and FFN skipping (Xu et al., 2025) select a subset of tokens to involve in attention or FFN computation and ignore the rest, decreasing latency while maintaining accuracy without dropping context tokens in forward propagation. Nevertheless, they still suffer from three key limitations: 1) *Insufficient structure optimization*. Existing methods are typically designed for either Multi-Head Attention (MHA) or

Feed Forward Network (FFN) modules that focuses on pursuing high acceleration ratios, which often induces severe performance degradation and hinders the overall speedup. 2) *Suboptimal token selection by outdated criteria.* To select crucial tokens for computation, most existing methods rely on outdated criteria such as attention score from preceding layers, which fail to reflect importance in the layer to be computed, thereby leading to suboptimal token skipping decisions. 3) *Over preservation of tokens introducing interference.* Retaining full context throughout deep layers is often unnecessary, as the redundant tokens require repeated evaluations for selection and diminish the discriminability between informative and uninformative tokens, thereby leading to biased selection.

To address the above limitations, we propose SPT, a training-free framework for efficient long-context LLM inference. Specifically, we first analyze the feasibility of token skipping across deep layers and emphasize our main principle of self-predictive token skipping: **A token’s eligibility for skipping is determined by its potential impact within the target layer.** Based on this insight, we design specific criteria to select active tokens for typical structures. As for MHA, we employ Partial Attention Probing (PAP) that estimates token contribution by probing a small portion of attention score. As for FFN, we propose Low-rank Transformation Probing (LTP) that pre-constructs a low-rank proxy network to approximate FFN, guiding token selection via proxy-induced variations combined with attention scores. To further improve efficiency and mitigate redundancy interference, a Multi-Stage Delayed Pruning (MSDP) strategy is developed, which divides layers into stages and applies pruning at stage boundaries after token skipping, thereby progressively reducing both active and candidate tokens.

In summary, our main contributions lie in three-fold:

- We propose SPTS, a novel training-free framework for accelerating long-context LLM inference, which achieves remarkable speedups in both prefilling and decoding phases.
- We design Partial Attention Probing (PAP) and Low-rank Transformation Probing (LTP) for MHA and FFN modules, respectively, by applying self-predictive information to boost token selection. We also develop a Multi-Stage Delayed Pruning (MSDP) strategy to suppress the redundancy-induced interference.
- We conduct extensive experiments on representative LLMs, showing that SPTS outperforms state-of-the-art approaches in both efficiency and accuracy. As shown in Fig. 1, our method achieves up to 2.46× and 2.29× speedups on LLaMA-3.1-8B-Instruct (Dubey et al., 2024) for prefilling and end-to-end generation, respectively, with minimal performance degradation.

## 2. Related Work

### 2.1. LLM Inference and Efficiency

Prevalent LLM inference involves two phases: prefilling and auto-regressive decoding (Zhao et al., 2023). During prefilling, the model processes the input sequence to generate the first token, computing full causal attention and storing the key and value representations in the Key-Value (KV) Cache. In decoding, each newly generated token is fed back as input and attends to the KV Cache to produce the next token. For long-context tasks with tens of thousands of input tokens (Bai et al., 2024), both phases pose significant challenges in inference efficiency (Xu et al., 2024).

FlashAttention (Dao, 2024) is a key baseline for efficient LLM deployment, accelerating MHA via optimized memory access. Sparse attention further reduces attention computation over long context (Lai et al., 2025; Jiang et al., 2024), but both schemes leave the computation-heavy FFN largely unoptimized. Token-level methods, such as token pruning (Xiao et al., 2024) and skipping (Xu et al., 2025), offer complementary acceleration and can be combined with FlashAttention for more comprehensive speedup.

### 2.2. Token Pruning

Token pruning reduces computation by shortening the sequence, with effectiveness depending on when it is applied. Prior works commonly focus on the decoding phase (KV Cache eviction) (Li et al., 2024a; Liu et al., 2025b; Qin et al., 2025; Su et al., 2025), yet at the cost of increased prefilling latency. Recognizing prefilling as a bottleneck, recent works shift pruning to this phase and design strategies to compensate for information loss. PyramidInfer (Yang et al., 2024) and GemFilter (Shi et al., 2024) enhance token selection by lengthening the pruning window and using extra forward passes, respectively, which adds non-negligible overhead. LazyLLM (Fu et al., 2024) and SlimInfer (Long et al., 2025) recompute the pruned tokens during decoding, leading to substantial generation slowdown. Overall, token pruning methods face an inherent trade-off between effective acceleration and faithful information preservation.

### 2.3. Token Skipping

Token skipping leverages the residual connections in modern network architectures to route a subset of tokens through shortcut paths only, thereby reducing computation while preserving sequence integrity. Early works either skip all tokens in fixed layers (Men et al., 2025) or employ learned predictors to determine which tokens to bypass (Li et al., 2024b). FTP (Xu et al., 2025) explores a training-free token skipping to accelerate FFN computation, but encounters limited speedup. Moreover, its attention-based criterion provides suboptimal token selection signals.

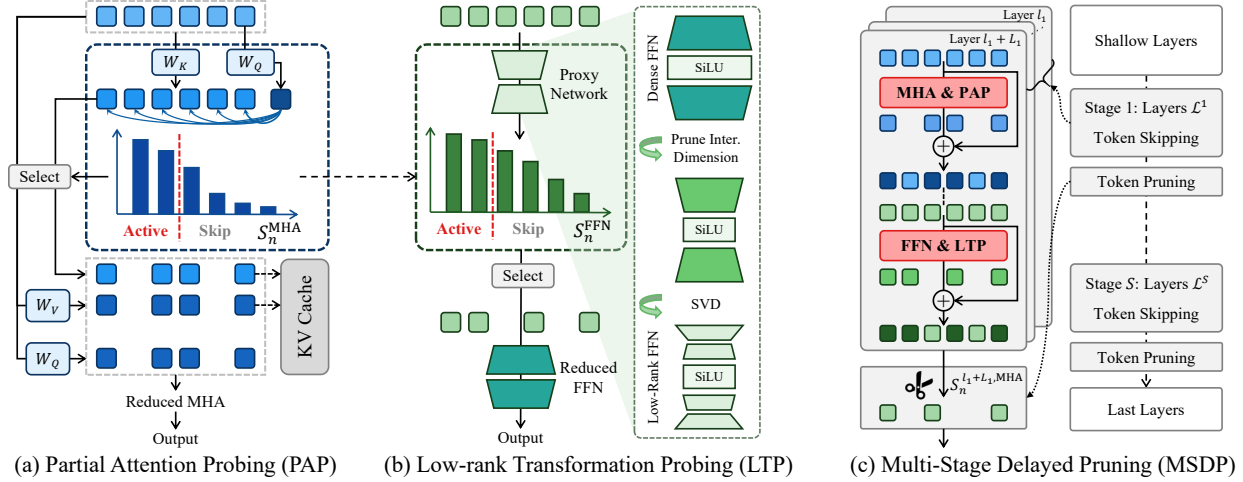


Figure 2. Framework overview of our proposed method. (a) Partial Attention Probing (PAP) performs token skipping in MHA by pre-computing a small fraction of attention to identify informative tokens, which then participate in reduced attention computation. (b) Low-rank Transformation Probing (LTP) enables token skipping in FFN by leveraging an offline-derived low-rank proxy network to probe token transformations, which are combined with attention-based information to guide token selection for reduced feed-forward. (c) Multi-Stage Delayed Pruning (MSDP) partitions the network into multiple stages, where the set of candidate tokens remains fixed within each stage and is reduced through pruning at stage boundaries.

In this work, we further explore token skipping strategies tailored for long-context LLMs, aiming to achieve more comprehensive and accurate acceleration.

### 3. Methodology

#### 3.1. Framework Overview

Most prevalent LLMs adopt the standard Transformer (Vaswani et al., 2017) architecture, where stacked MHA and FFN blocks dominate computational. Therefore, we target both to enable more aggressive acceleration.

Notably, the two blocks adopt a residual structure with shortcut connections. Without loss of generality, let  $\mathcal{F}(\cdot) \in \{\mathcal{F}_{\text{MHA}}(\cdot), \mathcal{F}_{\text{FFN}}(\cdot)\}$  represent either the MHA or FFN computation, and denote the input and output hidden states of a block as  $\mathbf{X}$ ,  $\mathbf{Y} \in \mathbb{R}^{N \times D}$ , where  $N$  is the sequence length and  $D$  is the feature dimension. The block-wise computation can be formally expressed as:

$$\mathbf{Y} = \mathbf{X} + \mathcal{F}(\mathbf{X}). \quad (1)$$

Empirically, as shown in Fig. 3(a),  $\mathbf{X}$  and  $\mathbf{Y}$  exhibits increasing similarity in deep layers across both blocks, undergoing only minor transformations. This indicates that the residual shortcut preserves most context information and motivates skipping  $\mathcal{F}(\cdot)$  for a subset of tokens in each block.

Concretely, let  $\mathcal{T} = \{1, 2, \dots, N\}$  denote the candidate token indices of  $\mathbf{X}$  along the sequence dimension. A subset of active tokens  $\mathcal{T}_{\text{active}} \subset \mathcal{T}$  is selected, with cardinality  $|\mathcal{T}_{\text{active}}| = M$ . Then, the corresponding hidden states form

a reduced matrix  $\hat{\mathbf{X}} = \mathbf{X}[\mathcal{T}_{\text{active}}, :] \in \mathbb{R}^{M \times D}$ , which is processed exclusively by  $\mathcal{F}(\cdot)$ , while all remaining tokens follow an identity mapping, as formalized in Eq. (2).

$$\begin{aligned} \hat{\mathbf{Y}}[\mathcal{T}_{\text{active}}, :] &= \hat{\mathbf{X}} + \mathcal{F}(\hat{\mathbf{X}}), \\ \hat{\mathbf{Y}}[\mathcal{T}/\mathcal{T}_{\text{active}}, :] &= \mathbf{X}[\mathcal{T}/\mathcal{T}_{\text{active}}, :]. \end{aligned} \quad (2)$$

Building on this, our SPTS operates in the prefilling phase to enable inference-time acceleration. As illustrated in Fig. 2, full computation is retained in shallow layers to preserve complex information processing, while token skipping is applied in deeper layers. To address the aforementioned challenges, we introduce PAP and LTP for self-predictive selection of  $\mathcal{T}_{\text{active}}$ , and design the MSDP strategy to regulate the overall token flow. Notably, SPTS also compresses the KV Cache during MHA skipping, enabling speedup in both prefilling and decoding phases at once. The detailed inference procedure is summarized in Algorithm 1.

#### 3.2. Partial Attention Probing for MHA

Empirically, MHA blocks propagate information forward via causal attention, and prior studies suggest that most information diffusion occurs in shallow layers (Long et al., 2025). Here, we analyze the role of deep-layer MHA. As shown in Fig. 3(b), halting updates for almost all context tokens in deep MHA has little impact on model performance, whereas stopping the last-token update causes a significant drop. This indicates that deep MHA primarily serves to aggregate preceding token information into the last token, supporting subsequent content generation.

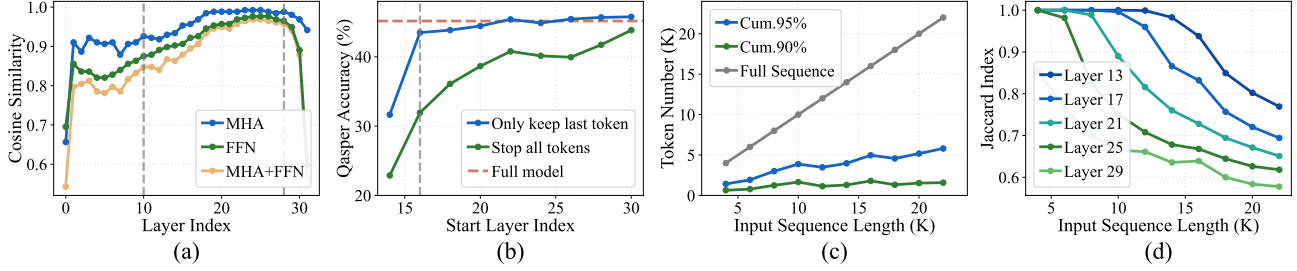


Figure 3. Empirical observations on LLaMA-3.1-8B-Instruct. (a) Layer-wise average cosine similarity of tokens before and after MHA, FFN, and the full Transformer block (MHA+FFN). (b) Accuracy fluctuations induced by disabling MHA updates for all input tokens, or for all of them except the last, starting from a given layer. (c) Number of tokens contributing to 90% and 95% of cumulative attention across deep layers for input sequences of varying lengths. (d) Jaccard index between consecutive-layer token sets selected via the attention criterion under a progressively reduced token budget, across distinct input lengths.

Accordingly, under a fixed computation budget, MHA token skipping can be formulated as the optimization problem in Eq. (3), minimizing information loss in the last token.

$$\hat{\mathcal{T}}_{\text{active}}^{\text{MHA}} = \arg \min_{\mathcal{T}_{\text{active}} \subset \mathcal{T}, |\mathcal{T}_{\text{active}}| = M} \|\hat{\mathbf{Y}}_N - \mathbf{Y}_N\|_2. \quad (3)$$

However, this problem is NP-hard, rendering exact solutions infeasible within a single forward propagation. Noting that attention mechanisms explicitly capture the information flow, we probe a lightweight, attention-based signal as a practical surrogate to approximate each token’s contribution and guide the token skipping process.

Specifically, prior to the target  $\mathcal{F}_{\text{MHA}}(\cdot)$ , we first compute the key projections for all tokens as  $\mathbf{K} = \mathbf{X}\mathbf{W}_K$ , and the query projection only for the last token as  $\mathbf{q} = \mathbf{X}_N\mathbf{W}_Q$ , where  $\mathbf{W}_Q$  and  $\mathbf{W}_K$  are projection matrices. Then, the Softmax-normalized attention scores between  $\mathbf{q}$  and  $\mathbf{K}$  are calculated and averaged across all heads to derive a token-wise contribution score, formally given by:

$$S_n^{\text{MHA}} = \frac{1}{H} \sum_{h=1}^H \text{Softmax}\left(\frac{\mathbf{q}_h \mathbf{K}_h^T}{\sqrt{d}}\right)[n], \quad (4)$$

where  $H$  and  $d$  denote the number of attention heads and the dimensionality per head, respectively. Accordingly, the top- $M$  tokens are selected, yielding the active indices as:

$$\mathcal{T}_{\text{active}}^{\text{MHA}} = \text{TopK}(\{S_n^{\text{MHA}}\}_{n=1}^N, M). \quad (5)$$

Finally, for a reduced  $\mathcal{F}_{\text{MHA}}(\cdot)$ , query and value projections are computed only for the selected tokens  $\hat{\mathbf{X}}$ , while the corresponding key projections are retrieved from the precomputed  $\mathbf{K}$  as  $\mathbf{K}[\mathcal{T}_{\text{active}}, :]$ . This further reduces the subsequent cost of causal attention and output projection.

Moreover, this MHA skipping strategy also enables on-the-fly KV Cache compression during prefilling. As Fig. 2(a) shows, only the key and value projections of active tokens

are cached, whereas the skipped tokens can still contribute in subsequent layers. Such selective caching reduces memory footprint and computational overhead in decoding, while providing a more flexible KV Cache management that helps preserve inference accuracy, as further discussed in Sec. B.

### 3.3. Low-rank Transformation Probing for FFN

Unlike the inter-token information propagation in MHA, FFN blocks perform independent representation refinement in an intra-token manner, which can be formulated as:

$$\mathcal{F}_{\text{FFN}}(\mathbf{X}) = (\sigma(\mathbf{X}\mathbf{W}_{\text{gate}}) \odot \mathbf{X}\mathbf{W}_{\text{up}})\mathbf{W}_{\text{down}}^T, \quad (6)$$

where  $\mathbf{W}_{\text{up}}, \mathbf{W}_{\text{gate}}, \mathbf{W}_{\text{down}} \in \mathbb{R}^{D \times D_{\text{ff}}}$  are the projection matrices with intermediate dimension  $D_{\text{ff}}$ ,  $\sigma$  is a non-linear activation (*e.g.* SiLU), and  $\odot$  is element-wise multiplication.

Accordingly, the objective of token skipping in FFN is to minimize the representation discrepancy over the sequence. Given Eq. (1) and the token-wise independence property, *i.e.*,  $\mathcal{F}_{\text{FFN}}(\mathbf{X})[n] = \mathcal{F}_{\text{FFN}}(\mathbf{X}_n)$ , the objective can be derived as Eq. (7). This formulation suggests that the transformation magnitude of each token serve as an effective criterion, whereby tokens undergoing larger representation changes should be selected as the active subset.

$$\begin{aligned} \hat{\mathcal{T}}_{\text{active}}^{\text{FFN}} &= \arg \min_{\mathcal{T}_{\text{active}} \subset \mathcal{T}, |\mathcal{T}_{\text{active}}| = M} \|\hat{\mathbf{Y}} - \mathbf{Y}\|_2 \\ &= \arg \max_{\mathcal{T}_{\text{active}} \subset \mathcal{T}, |\mathcal{T}_{\text{active}}| = M} \sum_{n \in \mathcal{T}_{\text{active}}} \|\mathcal{F}(\mathbf{X}_n)\|_2. \end{aligned} \quad (7)$$

**Low-rank Proxy FFN** However, probing the exact solution of Eq. (7) during online inference is computationally prohibitive, as it contradicts the goal of minimizing the inference cost of  $\mathcal{F}_{\text{FFN}}(\cdot)$  itself. Therefore, we adopt a lightweight proxy sub-network  $f(\cdot)$  to estimate token-wise transformations. For accurate prediction,  $f(\cdot)$  is explicitly designed to closely mimic the behavior of the original FFN:

$$\hat{f}(\cdot) = \arg \min_{f(\cdot)} \|\mathcal{F}_{\text{FFN}}(\mathbf{X}) - f(\mathbf{X})\|_2. \quad (8)$$

Inspired by network pruning methods (Sun et al., 2023; Wu et al., 2025), we construct  $f(\cdot)$  by initializing it from the original  $\mathcal{F}_{\text{FFN}}(\cdot)$  and slimming it via structured removal of projection matrix dimensions that have minimal impact.

Building on Eq. (6), we first reduce the intermediate dimension  $D_{\text{ff}}$  to  $D_{\text{low}}$  via a data-driven scheme. By forwarding a set of calibration text sequences through the model, we collect the hidden states immediately preceding  $\mathcal{F}_{\text{FFN}}(\cdot)$  to form a calibration token set  $\mathcal{G}$ . For each token  $\mathbf{x} \in \mathcal{G}$ , we compute its activation saliency vector as

$$z(\mathbf{x}) = |\sigma(\mathbf{x}\mathbf{W}_{\text{gate}}) \odot \mathbf{x}\mathbf{W}_{\text{up}}| \in \mathbb{R}^{D_{\text{ff}}}. \quad (9)$$

The importance of the  $j$ -th dimension is then estimated by averaging the top- $\rho$  fraction of its saliency values across  $\mathcal{G}$ , yielding the final importance score:

$$I_j = \text{Mean}(\text{TopK}(\{z(\mathbf{x})[j] \mid \mathbf{x} \in \mathcal{G}\}, \rho \times |\mathcal{G}|)). \quad (10)$$

Intuitively, this criterion prioritizes intermediate dimensions that are consistently highly activated by the responsive tokens, thus preserving the most informative channels. Accordingly, we select the top- $D_{\text{low}}$  dimensions  $\mathcal{C} = \text{TopK}(\{I_j\}_{j=1}^{D_{\text{ff}}}, D_{\text{low}})$  and construct the reduced projection matrices as:

$$\mathbf{W}' = \mathbf{W}[:, \mathcal{C}], \forall \mathbf{W} \in \{\mathbf{W}_{\text{gate}}, \mathbf{W}_{\text{up}}, \mathbf{W}_{\text{down}}\}. \quad (11)$$

However, dense matrix multiplications with  $\mathbf{W}'$  remain costly. To further reduce computation, we apply a low-rank factorization. Concretely, we perform a Singular Value Decomposition (SVD) on  $\mathbf{W}'$  and retain the top- $r$  singular values, yielding a rank- $r$  approximation  $\mathbf{W}' \approx \mathbf{U}\mathbf{V}$ , where  $\mathbf{U} \in \mathbb{R}^{D \times r}$  and  $\mathbf{V} \in \mathbb{R}^{r \times D_{\text{low}}}$  with  $r \ll \min(D, D_{\text{low}})$ .

Finally, by integrating the two dimensionality reduction steps, the computation of proxy  $f(\cdot)$  can be formalized as:

$$\begin{aligned} f(\mathbf{X}) &= (\text{Gate}(\mathbf{X}) \odot \text{Up}(\mathbf{X}))\mathbf{V}_{\text{down}}^T \mathbf{U}_{\text{down}}^T, \\ \text{Gate}(\mathbf{X}) &= \sigma(\mathbf{X}\mathbf{U}_{\text{gate}} \mathbf{V}_{\text{gate}}), \text{Up}(\mathbf{X}) = \mathbf{X}\mathbf{U}_{\text{up}} \mathbf{V}_{\text{up}}. \end{aligned} \quad (12)$$

**Conditioned Transformation for Token Selection** According to Eqs. (7) and (12), the influence of an FFN block on each token  $C_n^{\text{FFN}}$  can be estimated via the  $l_2$ -norm of its output from the proxy network:

$$C_n^{\text{FFN}} = \|f(\mathbf{X}_n)\|_2, \quad (13)$$

which identifies tokens whose representations undergo the largest transformations and should therefore be prioritized for active computation rather than skipped.

However, such token-independent estimation ignores task-related dependencies: some tokens may have small self-updates yet encode crucial information, and skipping them

aggressively may introduce undesirable noise. To address this, we skip tokens only when they are both minimally informative and undergo limited changes, *i.e.* exhibiting low transformation conditioned on a low information score.

Formally, we incorporate the probed contribution score from Eq. (4) to capture task relevance. The two metrics are combined via multiplicative fusion to define a conditioned transformation score as Eq. (14), and the active token set is ultimately determined by a top- $M$  selection as Eq. (15).

$$S_n^{\text{FFN}} = C_n^{\text{FFN}} \cdot S_n^{\text{MHA}}. \quad (14)$$

$$\mathcal{T}_{\text{active}}^{\text{FFN}} = \text{TopK}(\{S_n^{\text{FFN}}\}_{n=1}^N, M). \quad (15)$$

### 3.4. Multi-Stage Delayed Token Pruning

For clarity in this section, we use  $l$  to denote the layer index, and all variables in Secs. 3.2 and 3.3 are instantiated in a layer-wise manner, *e.g.*  $\mathcal{T}^l, \mathcal{T}_{\text{active}}^l$  for the candidate and active sets, and  $M^l$  for the number of active tokens.

As observed in Fig. 3(a), tokens exhibit diminishing update magnitudes and increasing stability across blocks with depth, motivating a non-uniform token skipping strategy across layers. Following the prior empirical evidence that informative tokens do not scale with sequence length in long-context settings (Shi et al., 2024; Long et al., 2025), we adopt a fixed token budget at each layer rather than a fixed pruning ratio, enabling more consistent preservation of critical information. Concretely, the number of activate tokens is constrained by  $M^l = \min(|\mathcal{T}^l|, M_{\text{fixed}}^l)$ , where  $M_{\text{fixed}}^l$  is a predefined budget.

Furthermore, while retaining all context tokens as candidates intuitively preserves the primary information flow, doing so in deep layers leads to increasingly imbalanced trade-off between probing overhead and actual computation savings, especially under fixed token budgets.

More critically, due to the normalization property of attention, retaining excessive tokens in long sequences induces a smoothing effect on score distributions, degrading reliable top-token selection. As shown in Fig. 3(c), accumulating 90% of attention mass in all deep layers requires only a fixed number of tokens, whereas achieving higher coverage demands increasingly more tokens as sequence length grows, reflecting score dilution. Moreover, Fig. 3(d) shows that under non-uniform budgets, longer sequences exhibit lower top-token consistency across adjacent deep layers, indicating increased interference from redundant tokens.

To address these issues, we introduce delayed pruning on top of token skipping to progressively remove redundant tokens. The skipping layers are divided into multiple stages, each followed by a pruning step at its last layer. Formally, let  $\mathcal{L}^s = \{l_s, l_s + 1, \dots, l_s + L_s\}$  denote the  $L_s$  consecutive

## Probe and Skip: Self-Predictive Token Skipping for Efficient Long-Context LLM Inference

Table 1. Comparison of performance scores and TTFT acceleration ratios (TTFT ratio) by various methods for three representative LLMs on the LongBench dataset. The best results are highlighted in **bold** and the second-best ones are underlined.

Method	Single-Doc. QA		Multi-Doc. QA			Summarization				Few-shot Learning			Synthetic Task		Code Completion		Avg. (%)	TTFT ratio	
	Qasper	MQA	HPQA	2Wiki	MuSiQue	GovRep	QMSum	MNews	VCSum	TREC	TQA	SAMSum	LSHT	Count	PassR	LCC			RepB-p
<i>LLaMA-3.1-8B-Instruct</i>																			
Full Model	45.16	54.71	55.64	44.73	30.66	34.99	25.26	27.17	17.16	72.50	91.66	43.98	46.50	7.00	99.50	63.02	56.01	47.98	1.00×
LazyLLM	<b>45.56</b>	53.17	53.47	45.50	30.44	32.76	24.84	26.19	16.99	71.00	91.25	43.28	46.00	<b>7.50</b>	<b>99.50</b>	58.66	55.17	47.13	1.63×
MInference	44.59	52.64	53.51	<b>47.30</b>	28.08	<b>35.25</b>	<b>25.51</b>	<b>27.29</b>	<b>17.43</b>	<b>72.50</b>	91.42	43.58	<u>46.50</u>	6.55	95.50	63.30	<u>57.41</u>	47.55	0.47×
FlexPrefill	<u>45.18</u>	<b>55.52</b>	<b>56.95</b>	42.75	<u>32.14</u>	<u>34.55</u>	<u>25.16</u>	26.86	17.39	71.00	90.74	43.50	42.00	3.16	81.50	62.93	<b>60.89</b>	46.60	0.96×
SlimInfer	<u>45.18</u>	53.72	54.34	43.68	30.69	34.40	24.60	<u>27.28</u>	16.94	71.00	<u>91.64</u>	<b>44.63</b>	45.50	6.40	98.50	<u>63.38</u>	56.63	<u>47.56</u>	1.62×
PyramidInfer	44.02	54.22	53.75	44.49	30.39	33.98	24.64	26.06	<u>17.41</u>	68.00	90.98	43.58	46.00	5.97	<b>99.50</b>	<b>63.57</b>	57.04	47.27	1.19×
FTP	37.79	48.49	49.68	40.08	29.41	22.12	23.75	24.14	14.32	64.50	87.04	39.05	37.00	1.85	98.50	51.87	45.41	42.06	1.32×
GemFilter	44.65	52.48	<u>55.84</u>	45.42	<b>32.15</b>	33.53	22.12	27.11	16.56	70.50	<b>92.05</b>	43.19	<b>50.00</b>	5.31	<b>99.50</b>	59.90	50.20	47.09	1.31×
<b>SPTS (Ours)</b>	44.98	<u>55.37</u>	<u>53.66</u>	<u>46.69</u>	30.43	33.49	24.73	27.10	16.76	<b>72.50</b>	<u>91.64</u>	<u>44.23</u>	<u>46.50</u>	<u>7.24</u>	99.00	63.14	55.20	<b>47.80</b>	<b>1.68×</b>
<i>Qwen-2.5-7B-Instruct</i>																			
Full Model	43.92	52.76	57.97	46.56	30.16	31.78	23.36	24.30	16.05	72.50	88.64	45.64	43.00	8.00	100.0	60.44	66.84	47.76	1.00×
LazyLLM	39.79	45.71	53.30	42.58	28.94	31.16	23.08	23.28	15.61	66.50	87.67	45.31	42.25	6.59	<b>100.0</b>	57.46	63.89	45.48	1.28×
MInference	43.61	<b>52.32</b>	<b>57.59</b>	45.31	<u>30.48</u>	<u>31.72</u>	<u>23.36</u>	<b>24.10</b>	15.85	<b>72.50</b>	<b>89.61</b>	<b>46.33</b>	42.10	<b>9.00</b>	91.50	59.88	<b>66.84</b>	47.18	0.41×
FlexPrefill	41.87	50.89	56.31	41.53	29.43	<b>31.92</b>	<b>23.66</b>	23.92	<u>15.92</u>	71.50	88.93	45.73	33.80	3.00	75.50	<b>60.08</b>	62.47	44.50	0.90×
SlimInfer	<u>43.70</u>	<u>52.14</u>	<u>57.57</u>	<u>47.01</u>	27.83	31.32	23.24	23.85	<b>15.96</b>	<u>72.00</u>	88.56	45.55	<b>43.50</b>	<b>9.00</b>	99.00	59.74	<u>66.36</u>	<u>47.43</u>	<u>1.34×</u>
PyramidInfer	37.09	45.85	54.88	44.88	29.01	30.23	23.05	22.82	15.34	63.50	<u>89.43</u>	46.26	42.25	8.50	<b>100.0</b>	<u>59.99</u>	66.25	45.84	1.16×
FTP	41.09	48.37	53.65	36.45	20.75	28.05	22.23	21.99	15.33	65.50	89.23	43.88	36.50	6.50	98.50	59.57	64.69	44.25	<b>1.36×</b>
GemFilter	42.28	44.34	52.12	46.54	22.82	30.46	19.79	23.85	15.22	68.00	88.31	43.26	41.25	5.50	97.50	59.79	65.05	45.06	1.30×
<b>SPTS (Ours)</b>	<b>44.06</b>	51.29	56.66	<b>47.37</b>	<b>32.44</b>	30.92	22.96	<u>23.94</u>	15.72	70.50	89.04	<u>46.19</u>	<u>43.25</u>	8.00	<b>100.0</b>	59.68	65.47	<b>47.50</b>	<b>1.36×</b>
<i>openPangu-Embedded-1B-V1.1*</i>																			
Full Model	27.85	44.15	32.17	34.75	17.78	26.62	19.68	22.78	14.56	67.00	79.70	38.96	33.17	2.62	15.50	25.37	25.80	31.09	1.00×
PyramidInfer	<u>25.05</u>	39.21	<u>30.05</u>	<u>30.87</u>	<u>15.54</u>	24.64	18.88	21.42	14.32	<u>64.50</u>	<b>79.10</b>	<b>38.59</b>	<b>34.31</b>	1.33	14.50	23.78	<u>25.21</u>	<u>29.49</u>	0.83×
FTP	23.03	<u>39.22</u>	23.78	25.61	10.31	23.62	<b>19.82</b>	19.99	14.33	60.00	76.03	36.00	28.57	<u>2.17</u>	14.00	20.28	18.09	26.76	0.87×
GemFilter	21.88	37.96	24.36	29.09	13.36	<u>24.66</u>	18.38	<u>22.67</u>	<b>14.74</b>	62.00	77.81	35.16	<u>34.29</u>	<b>2.64</b>	<b>24.25</b>	<b>25.83</b>	<b>28.19</b>	29.25	<u>1.24×</u>
<b>SPTS (Ours)</b>	<b>26.44</b>	<b>43.83</b>	<b>32.56</b>	<b>36.22</b>	<b>16.50</b>	<b>24.82</b>	<u>19.02</u>	<b>22.72</b>	<u>14.63</u>	<b>66.50</b>	<u>79.05</u>	<u>38.32</u>	33.50	1.00	<u>15.00</u>	<u>25.49</u>	24.96	<b>30.62</b>	<b>1.32×</b>

\* The speed of openPangu are reported by adopting the original Ascend CANN runtime and operator kernels, which can be further improved by specific optimizations.

layers forming the  $s$ -th stage. All layers  $l \in \mathcal{L}^s$  share the same candidate token set  $\mathcal{T}^l$  of size  $N_s$ . At the end of stage  $s$ , *i.e.* after layer  $l_s + L_s$ , tokens are pruned based on the last contribution scores  $S_n^{l_s+L_s, \text{MHA}}$  as Eq. (4). This yields a reduced candidate set forwarding to the subsequent layers:

$$\mathcal{T}^l = \text{TopK}(\{S_n^{l_s+L_s, \text{MHA}}\}_{n=1}^{N_s}, N_{s+1}), \forall l \in \mathcal{L}^{s+1}. \quad (16)$$

## 4. Experimental Results and Analysis

### 4.1. Experimental Settings

**Models** Following prior works (Xu et al., 2025; Shi et al., 2024) and recent advances in long-context LLMs, we evaluate SPTS on three representative models: the large-scale LLaMA-3.1-8B-Instruct (Dubey et al., 2024), Qwen-2.5-7B-Instruct (Team, 2024), and the more compact openPangu-

Embedded-1B-V1.1(Chen et al., 2025), which are referred to as LLaMA, Qwen and openPangu, respectively.

**Datasets and Evaluation Metrics** To evaluate the effectiveness of our method, we conduct experiments on the LongBench (Bai et al., 2024) dataset, a comprehensive benchmark for long-context inference comprising 17 sub-datasets across 6 major task categories. Concretely, following the official evaluation protocols, we report the F1 score for the Single- and Multi-Document QA tasks including Qasper, MultiFieldQA (MQA), HotpotQA (HPQA), 2WikiMultihopQA (2Wiki), MuSiQue; the Rouge-L score (Lin, 2004) for Summarization tasks including GovReport (GovRep), QMSum, MultiNews (MNews) and VCSUM; the exact match Accuracy (%) for Synthetic tasks including PassageCount (Count), PassageRetrieval (PassR); and the

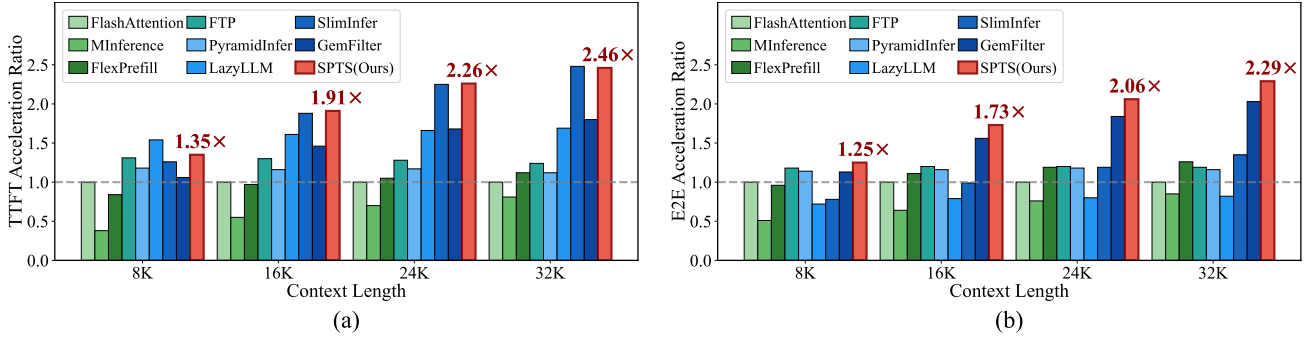


Figure 4. Comparison of (a) TTFT and (b) E2E acceleration ratios with different methods across distinct context lengths on LLaMA.

Edit Sim (Levenshtein distance) (Svyatkovskiy et al., 2020) for Code Completion tasks including LCC, RepoBench-P (RepB-p). For Few-shot Learning tasks, we present the classification Accuracy (%) on TREC and LSHT, the F1 score on TriviaQA (TQA), and the Rouge-L score on SAM-Sum. Moreover, we report the average performance over all subsets, referred to as Avg. (%). To evaluate inference efficiency, by following (Long et al., 2025), we measure both the time to first token (TTFT) and the end-to-end (E2E) latency for decoding 16 tokens, and report the speedups via dividing the latency of the full model by the counterpart of each method, referred to as the TTFT Acceleration Ratio and the E2E Acceleration Ratio, respectively.

**Implementation Details** We implement all methods on top of the Transformers library (Wolf et al., 2019), with FlashAttention (Dao, 2024) maintained as the baseline for inference acceleration. For LLaMA (32 layers), token skipping is enabled from layer 10. The network is divided into four stages with boundaries after layers (13, 18, 23, 28). The fixed active token budgets  $M_{\text{fixed}}^l$  for each stage are set to (9, 7, 4, 2)K (1K = 1024 tokens), and the candidate token set is further pruned by 1K tokens at the end of each stage. For Qwen (28 layers), token skipping starts from layer 9. Four stages are defined ending at layers (12, 16, 20, 24), using active token budgets of (13, 10, 7, 4)K, while stage-end pruning removes 2K tokens to form the candidate set. For openPangu (26 layers), token skipping begins at layer 11. The model is partitioned at layers (13, 16, 19, 22), with active token budgets of (13, 10, 7, 4)K, and candidate token sets reduced by 2K tokens after each stage. In the LTP module, we set the  $(D_{\text{low}}, r)$  pairs to (512, 192), (1024, 256) and (1024, 128) for LLaMA, Qwen and openPangu, respectively, according to their FFN scales. For Eq. (10), we sample 200 text sequences from the Qasper subset of LongBench as calibration data, and  $\rho$  is fixed to 0.2 for all experiments. All experiments for LLaMA and Qwen are conducted on a single NVIDIA A800 GPU (80 GB). For openPangu, experiments are conducted on one Ascend

910B2 NPU (64GB).

## 4.2. Main Results on Accuracy-Efficiency Trade-off

We compare our proposed SPTS with state-of-the-art long-context LLM acceleration methods. MInference (Jiang et al., 2024) and FlexPrefill (Lai et al., 2025) explore sparse attention, PyramidInfer (Yang et al., 2024), GemFilter (Shi et al., 2024), LazyLLM (Fu et al., 2024) and SlimInfer (Long et al., 2025) are token pruning methods, and FTP (Xu et al., 2025) implements token skipping. As most methods primarily target speedup in prefilling, we conduct comparisons under comparable average TTFT acceleration ratios for fairness.

**On Accuracy** As shown in Tab. 1, our method consistently achieves higher average scores while delivering more substantial TTFT speedups. Specifically, SPTS outperforms the second-best methods by 0.24%, 0.07% and 1.13% on LLaMA, Qwen and openPangu, respectively. Notably, while SlimInfer is competitive in both accuracy and TTFT acceleration, it suffers from pronounced degradation in decoding speed, as discussed below. GemFilter and PyramidInfer prune tokens directly during prefilling, potentially discarding critical contextual information and causing performance degradation. FTP supports token skipping but relies on outdated, redundancy-affected selection criteria, thus leading to significant accuracy loss under high acceleration ratios. Overall, by enabling more comprehensive token skipping and leveraging more informative token selection signals, SPTS preserves and extracts critical information from long sequences more effectively without heavy auxiliary operations. The consistent improvements across models of varying structures, scales, and hardware platforms further highlight the strong generalization capability of our approach.

**On Efficiency** Following (Long et al., 2025), we sample input sequences of four different lengths (8K, 16K, 24K and 32K) from LongBench (Bai et al., 2024) to evaluate inference efficiency. For each context length, 20 distinct sequences are sampled, and the corresponding latencies are

Table 2. Ablation of the PAP, LTP and MSDP modules on TTFT acceleration ratios across varying context lengths with LLaMA.

Method	8K	16K	24K	32K
Full Model	1.00×	1.00×	1.00×	1.00×
+ PAP	1.08×	1.24×	1.35×	1.44×
+ PAP + LTP	1.26×	1.70×	1.98×	2.15×
+ PAP + LTP + MSDP	<b>1.35×</b>	<b>1.91×</b>	<b>2.26×</b>	<b>2.46×</b>

Table 3. Effect of the PAP module on KV Cache memory savings across varying context lengths with LLaMA.

Method	8K	16K	24K	32K
Ours w/o PAP (Full Cache)	4.00	8.00	12.00	16.00
Ours w/ PAP	2.81	4.13	5.38	6.63
Memory Saving (%)	<b>29.7</b>	<b>48.4</b>	<b>55.2</b>	<b>58.6</b>

recorded and averaged following a warmup period. We evaluate both TTFT and E2E acceleration ratios across different methods, with the full model using dense FlashAttention (Dao, 2024) as the baseline. As shown in Fig. 4, SPTS consistently accelerates both the prefilling and decoding phases, with speedups increasing as the context length grows. At a length of 32K, it achieves 2.46× and 2.29× acceleration for TTFT and E2E latencies, respectively. Importantly, these efficiency gains are obtained while maintaining state-of-the-art average accuracy in Tab. 1, highlighting its significant efficiency potential in long-context inference scenarios.

### 4.3. Ablation Study

**On Main Components** We evaluate the efficiency contributions of the main components: the Partial Attention Probing (PAP) for MHA, the Low-rank Transformation Probing (LTP) for FFN, and the Multi-Stage Delayed Pruning (MSDP) strategy. As shown in Tab. 2, sequentially incorporating PAP and LTP enables skipping more computations, achieving cumulative speedups of 1.44× and 2.15×. The introduction of MSDP further improves efficiency by reducing the token selection overhead, ultimately yielding a total speedup of 2.46× for a 32K context length.

**On PAP** We analyze the effect of the PAP design. As shown in Tab. 3, incorporating PAP reduces the KV Cache memory footprint while maintaining token forward propagation in prefilling. For a 32K context, it achieves up to 58.6% memory savings. This demonstrates that our method not only exploits FFN-level token skipping as FTP (Xu et al., 2025) but also provides an advantage in memory efficiency.

**On LTP** We further analyze the effect of the proxy network in the LTP module. To isolate its effect, we only apply token skipping to FFN blocks, with 40% of tokens skipped in all deep layers. As shown in Tab. 4, only utilizing

Table 4. Effect of low-rank proxy network on LLaMA. Results are reported on five representative LongBench subsets and the average score (Avg.) on the full dataset.

Skipping Criterion	Dataset					Avg. (%)
	MQA	HPQA	SAMSum	Count	RepB-p	
$S_n^{\text{MHA}}$	52.96	53.39	44.23	5.59	52.79	46.31
$C_n^{\text{FFN}} \cdot S_n^{\text{MHA}}$	<b>53.71</b>	<b>54.11</b>	<b>44.64</b>	<b>7.47</b>	<b>53.26</b>	<b>46.85</b>

Table 5. Effect of Delayed Pruning (DP) on LLaMA across five LongBench subsets and average (Avg.) on the full dataset.

Method	Dataset					Avg. (%)
	MQA	HPQA	SAMSum	Count	RepB-p	
Ours w/o DP	54.99	52.51	43.72	4.32	52.39	46.11
Ours w/ DP	<b>55.37</b>	<b>53.66</b>	<b>44.23</b>	<b>7.24</b>	<b>55.20</b>	<b>47.80</b>

the attention-based contribution scores from the preceding MHA block, *i.e.* Eq. (4), provides a reasonable token selection. However, incorporating the low-rank proxy network  $f(\cdot)$  with a conditioned transformation criterion as Eq. (14) enables prediction of token-wise response to the target FFN block, preserving those expected to undergo substantial updates. This leads to more accurate active token selection and consistent performance gains across tasks, with an average score improvement of 0.54%.

**On MSDP** We assess the effect of delayed pruning, as shown in Tab. 5. By applying pruning on top of token skipping, redundant tokens are gradually removed, improving both the accuracy and stability of token selection. This is particularly beneficial for long-sequence tasks such as HPQA and Count, where pruning mitigates the smoothing of selection scores induced by extended contexts. Overall, it yields an average score improvement of 1.69%.

## 5. Conclusion

In this work, we investigate token skipping-based acceleration for long-context LLM inference, and propose a novel training-free framework, dubbed SPTS. By introducing the Partial Attention Probing (PAP) and Low-rank Transformation Probing (LTP) modules, SPTS achieves comprehensive acceleration of the model’s predominant computational components while leveraging a self-predictive mechanism for more accurate token skipping. In addition, a Multi-Stage Delayed Pruning (MSDP) strategy is incorporated to allocate token budgets effectively and mitigate interference from redundant tokens. Extensive experiments on three representative long-context LLMs and two hardware platforms demonstrate that SPTS consistently improves inference latency while maintaining model accuracy, *e.g.* achieving 2.46× TTFT and 2.29× E2E speedups, highlighting its effectiveness and generalizability in long-context scenarios.

## Impact Statement

This paper presents work whose goal is to advance the field of Machine Learning. There are many potential societal consequences of our work, none which we feel must be specifically highlighted here.

## References

- Bai, Y., Lv, X., Zhang, J., Lyu, H., Tang, J., Huang, Z., Du, Z., Liu, X., Zeng, A., Hou, L., et al. Longbench: A bilingual, multitask benchmark for long context understanding. In *Proceedings of the Annual Meeting of the Association for Computational Linguistics*, volume 1, pp. 3119–3137, 2024.
- Chen, H., Wang, Y., Han, K., et al. Pangu embedded: An efficient dual-system llm reasoner with metacognition. *arXiv preprint arXiv:2505.22375*, 2025.
- Dao, T. Flashattention-2: Faster attention with better parallelism and work partitioning. In *Proceedings of the International Conference on Learning Representations*, 2024.
- Dubey, A., Jauhri, A., Pandey, A., Kadian, A., Al-Dahle, A., Letman, A., Mathur, A., Schelten, A., Yang, A., Fan, A., et al. The llama 3 herd of models. *arXiv preprint arXiv:2407.21783*, 2024.
- Fu, Q., Cho, M., Merth, T., Mehta, S., Rastegari, M., and Najibi, M. Lazyllm: Dynamic token pruning for efficient long context llm inference. In *Workshop on Efficient Systems for Foundation Models II@ ICML*, 2024.
- Jiang, H., Li, Y., Zhang, C., Wu, Q., Luo, X., Ahn, S., Han, Z., Abdi, A. H., Li, D., Lin, C.-Y., Yang, Y., and Qiu, L. MInference 1.0: Accelerating pre-filling for long-context LLMs via dynamic sparse attention. In *Advances in Neural Information Processing Systems*, 2024. URL <https://openreview.net/forum?id=fPBACAbqSN>.
- Lai, X., Lu, J., Luo, Y., Ma, Y., and Zhou, X. Flexprefill: A context-aware sparse attention mechanism for efficient long-sequence inference. In *Proceedings of the International Conference on Learning Representations*, 2025.
- Li, Y., Huang, Y., Yang, B., Venkitesh, B., Locatelli, A., Ye, H., Cai, T., Lewis, P., and Chen, D. Snapkv: Llm knows what you are looking for before generation. In *Advances in Neural Information Processing Systems*, volume 37, pp. 22947–22970, 2024a.
- Li, Z., Zheng, J., Liu, J., Liu, H., Zhu, H., Li, Z., Yang, F., Huang, H., Peng, J., Li, D., et al. Ftp: A fine-grained token-wise pruner for large language models via token routing. *arXiv preprint arXiv:2412.11494*, 2024b.
- Lin, C.-Y. Rouge: A package for automatic evaluation of summaries. In *Text summarization branches out*, pp. 74–81, 2004.
- Liu, J., Zhu, D., Bai, Z., He, Y., Liao, H., Que, H., Wang, Z., Zhang, C., Zhang, G., Zhang, J., et al. A comprehensive survey on long context language modeling. *arXiv preprint arXiv:2503.17407*, 2025a.
- Liu, T., Xu, C., and McAuley, J. Repobench: Benchmarking repository-level code auto-completion systems. In *Proceedings of the International Conference on Learning Representations*, 2024.
- Liu, X., Tang, Z., Dong, P., Li, Z., Liu, Y., Li, B., Hu, X., and Chu, X. Chunkkv: Semantic-preserving kv cache compression for efficient long-context llm inference. *arXiv preprint arXiv:2502.00299*, 2025b.
- Long, L., Yang, R., Huang, Y., Hui, D., Zhou, A., and Yang, J. Sliminfer: Accelerating long-context llm inference via dynamic token pruning. *arXiv preprint arXiv:2508.06447*, 2025.
- Ma, X., Fang, G., and Wang, X. Llm-pruner: On the structural pruning of large language models. In *Advances in Neural Information Processing Systems*, pp. 21702–21720, 2023.
- Men, X., Xu, M., Zhang, Q., Yuan, Q., Wang, B., Lin, H., Lu, Y., Han, X., and Chen, W. Shortgpt: Layers in large language models are more redundant than you expect. In *Findings of the Association for Computational Linguistics: ACL*, pp. 20192–20204, 2025.
- Qin, Z., Cao, Y., Lin, M., Hu, W., Fan, S., Cheng, K., Lin, W., and Li, J. Cake: Cascading and adaptive kv cache eviction with layer preferences. In *Proceedings of the International Conference on Learning Representations*, 2025.
- Shi, Z., Ming, Y., Nguyen, X.-P., Liang, Y., and Joty, S. Discovering the gems in early layers: Accelerating long-context llms with 1000x input token reduction. *arXiv preprint arXiv:2409.17422*, 2024.
- Su, Y., Qiu, Q., Zhou, Y., Li, J., Xia, Q., Li, P., Duan, X., Wang, Z., and Zhang, M. Calidrop: Kv cache compression with calibration. *arXiv preprint arXiv:2507.19906*, 2025.
- Sun, M., Liu, Z., Bair, A., and Kolter, J. Z. A simple and effective pruning approach for large language models. In *Proceedings of the International Conference on Learning Representations*, 2023.
- Svyatkovskiy, A., Deng, S. K., Fu, S., and Sundaresan, N. Intellicode compose: Code generation using transformer.

- In *Proceedings of the 28th ACM joint meeting on European software engineering conference and symposium on the foundations of software engineering*, pp. 1433–1443, 2020.
- Team, Q. Qwen2. 5: A party of foundation models, september 2024. URL <https://qwenlm.github.io/blog/qwen2,5>, 5 (4), 2024.
- Vaswani, A., Shazeer, N., Parmar, N., Uszkoreit, J., Jones, L., Gomez, A. N., Kaiser, Ł., and Polosukhin, I. Attention is all you need. *Advances in Neural Information Processing Systems*, 30, 2017.
- Wang, X., Salmani, M., Omid, P., Ren, X., Rezagholizadeh, M., and Eshaghi, A. Beyond the limits: A survey of techniques to extend the context length in large language models. *arXiv preprint arXiv:2402.02244*, 2024.
- Wolf, T., Debut, L., Sanh, V., Chaumond, J., Delangue, C., Moi, A., Cistac, P., Rault, T., Louf, R., Funtowicz, M., et al. Huggingface’s transformers: State-of-the-art natural language processing. *arXiv preprint arXiv:1910.03771*, 2019.
- Wu, Z., Chen, J., and Wang, Y. Unified knowledge maintenance pruning and progressive recovery with weight recalling for large vision-language models. In *Proceedings of the AAAI Conference on Artificial Intelligence*, volume 39, pp. 8550–8558, 2025.
- Xiao, G., Tian, Y., Chen, B., Han, S., and Lewis, M. Efficient streaming language models with attention sinks. In *Proceedings of the International Conference on Learning Representations*, 2024.
- Xu, G.-H., Ding, J., Ding, H., Xu, Z., and Zhang, K. Ftp: Efficient prefilling for long-context llm inference via ffn token pruning. *OpenReview.net*, 2025. URL <https://openreview.net/forum?id=fL8Zp8o6RL>.
- Xu, M., Yin, W., Cai, D., Yi, R., Xu, D., Wang, Q., Wu, B., Zhao, Y., Yang, C., Wang, S., et al. A survey of resource-efficient llm and multimodal foundation models. *arXiv preprint arXiv:2401.08092*, 2024.
- Yang, D., Han, X., Gao, Y., Hu, Y., Zhang, S., and Zhao, H. Pyramidinfer: Pyramid kv cache compression for high-throughput llm inference. In *Findings of the Association for Computational Linguistics ACL*, pp. 3258–3270, 2024.
- Yang, Z., Qi, P., Zhang, S., Bengio, Y., Cohen, W., Salakhutdinov, R., and Manning, C. D. Hotpotqa: A dataset for diverse, explainable multi-hop question answering. In *Proceedings of the Conference on Empirical Methods in Natural Language Processing*, pp. 2369–2380, 2018.
- Zhao, W. X., Zhou, K., Li, J., Tang, T., Wang, X., Hou, Y., Min, Y., Zhang, B., Zhang, J., Dong, Z., et al. A survey of large language models. *arXiv preprint arXiv:2303.18223*, 1(2), 2023.
- Zhong, M., Yin, D., Yu, T., Zaidi, A., Mutuma, M., Jha, R., Hassan, A., Celikyilmaz, A., Liu, Y., Qiu, X., et al. Qm-sum: A new benchmark for query-based multi-domain meeting summarization. In *Proceedings of the Conference of the North American Chapter of the Association for Computational Linguistics: Human Language Technologies*, pp. 5905–5921, 2021.

## A. Overall Algorithm of SPTS Inference Process

The detailed procedure of inference with SPTS for each auto-regressive forward propagation is summarized in Algorithm 1. Lines 7 ~ 17 describe the MHA token skipping with Partial Attention Probing (PAP), as illustrated in Fig. 2(a). Lines 21 ~ 27 present the FFN token skipping with Low-rank Transformation Probing (LTP), as displayed in Fig. 2(b). Lines 32 ~ 34 are the delayed pruning strategy, corresponding to Fig. 2(c). For clarity, we omit some standard operations that are orthogonal to our method, such as layer normalization, positional embedding, etc.

---

### Algorithm 1 Self-Predictive Token Skipping (SPTS)

---

**Input:** An LLM with  $L$  layers, consisting of standard MHA blocks  $\{\mathcal{F}_{\text{MHA}}^l\}_{l=1}^L$  and FFN blocks  $\{\mathcal{F}_{\text{FFN}}^l\}_{l=1}^L$ ; pre-constructed low-rank proxy networks  $\{f^l(\cdot)\}_{l=1}^L$ ; candidate token budgets  $\{N_s\}$  and active token budgets  $\{M_{\text{fixed}}^s\}$  for multiple stages; input hidden states  $\mathbf{X}$ , KV Cache  $Cache$ .

**Output:** Final hidden states  $\mathbf{X}$  for next token prediction, updated KV Cache  $Cache$ .

```

1 for  $l \leftarrow 1$  to  $L$  do
2     # Get current sequence length. All tokens are initially candidate for skipping.
3      $N \leftarrow \text{Get\_sequence\_length}(\mathbf{X})$ 
4      $skip \leftarrow \text{Is\_prefill\_phase}() \wedge \text{In\_skip\_layers}(l)$  # Whether token skipping is enabled at layer  $l$ .
5      $s \leftarrow \text{Get\_stage\_index}(l)$  # Get the stage index associated with layer  $l$ .
6     # Partial Attention Probing (PAP) for MHA.
7     if  $skip$  then
8         # Compute key projections for all tokens and query projection for the last token.
9          $\mathbf{K} \leftarrow \mathbf{X}\mathbf{W}_K, \mathbf{q} \leftarrow \mathbf{X}_N\mathbf{W}_Q$ 
10         $S^{\text{MHA}} \leftarrow \text{Mean\_softmax\_attention}(\mathbf{q}, \mathbf{K})$  # Predict token contribution scores with Eq. (4).
11        # Get token budget and select active token indices.
12         $m \leftarrow \min(N, M_{\text{fixed}}^s), \mathcal{T}_{\text{active}}^{\text{MHA}} \leftarrow \text{TopK}(S^{\text{MHA}}, m)$ 
13         $\hat{\mathbf{K}} \leftarrow \mathbf{K}[\mathcal{T}_{\text{active}}, :]$  # Gather computed key projections corresponding to active tokens.
14        # Extract active tokens and compute reduced query and value projections.
15         $\hat{\mathbf{X}} \leftarrow \mathbf{X}[\mathcal{T}_{\text{active}}, :], \hat{\mathbf{Q}} \leftarrow \hat{\mathbf{X}}\mathbf{W}_Q, \hat{\mathbf{V}} \leftarrow \hat{\mathbf{X}}\mathbf{W}_V$ 
16         $Cache \leftarrow Cache \cup (\hat{\mathbf{K}}, \hat{\mathbf{V}})$  # Save the active key-value pairs into KV Cache.
17         $\hat{\mathbf{O}} \leftarrow \mathcal{F}_{\text{MHA}}^l(\hat{\mathbf{Q}}, \hat{\mathbf{K}}, \hat{\mathbf{V}})$  # Perform reduced MHA computation over active tokens.
18         $\mathbf{X}[\mathcal{T}_{\text{active}}, :] \leftarrow \hat{\mathbf{X}} + \hat{\mathbf{O}}$  # Updated active token representations via residual connection.
19    else
20        # Standard MHA computation with residual connection.  $Cache$  is also updated.
21         $\mathbf{X} \leftarrow \mathbf{X} + \mathcal{F}_{\text{MHA}}^l(\mathbf{X}, Cache)$ 
22    # Low-rank Transformation Probing (LTP) for FFN.
23    if  $skip$  then
24         $\mathbf{o} \leftarrow f^l(\mathbf{X}), C^{\text{FFN}} \leftarrow \|\mathbf{o}\|_2$  # Predict token-wise transformation with Eq. (13).
25         $S^{\text{FFN}} \leftarrow S^{\text{MHA}} \times C^{\text{FFN}}$  # Compute the conditioned transformation scores with Eq. (14).
26        # Get token budget and select active token indices.
27         $m \leftarrow \min(N, M_{\text{fixed}}^s), \mathcal{T}_{\text{active}}^{\text{FFN}} \leftarrow \text{TopK}(S^{\text{FFN}}, m)$ 
28        # Select active tokens and perform reduced FFN computation.
29         $\hat{\mathbf{X}} \leftarrow \mathbf{X}[\mathcal{T}_{\text{active}}^{\text{FFN}}, :], \hat{\mathbf{O}} \leftarrow \mathcal{F}_{\text{FFN}}^l(\hat{\mathbf{X}})$ 
30         $\mathbf{X}[\mathcal{T}_{\text{active}}^{\text{FFN}}, :] \leftarrow \hat{\mathbf{X}} + \hat{\mathbf{O}}$  # Updated active token representations via residual connection.
31    else
32         $\mathbf{X} \leftarrow \mathbf{X} + \mathcal{F}(\mathbf{X})$  # Standard FFN computation with residual connection.
33    # Execute delayed pruning at stage boundaries.
34    if  $\text{Is\_stage\_end}(l, s)$  then
35        # Select candidate token indices for the next stage.
36         $m \leftarrow \min(N, N_{s+1}), \mathcal{T}^{l+1} \leftarrow \text{TopK}(S^{\text{MHA}}, m)$ 
37         $\mathbf{X} \leftarrow \mathbf{X}[\mathcal{T}^{l+1}, :]$  # Discard the redundant tokens and shrink the hidden state sequence.
38 return  $\mathbf{X}, Cache$ 

```

---

## B. Further Remark on KV Cache Flexibility

We summarize existing methods from the perspective of KV Cache management. As illustrated in Fig. 5, SPTS exhibits an additional advantage by striking a favorable accuracy-efficiency trade-off through flexible KV Cache compression. Specifically, as described in Sec. 3.2, by incorporating PAP for token skipping in MHA, the key and value projections are computed only for active tokens, which are subsequently stored in the KV Cache. This naturally enables an online KV Cache compression during the prefilling phase. Meanwhile, benefiting from the residual connections, tokens skipped at current layer are not permanently discarded, yet remain eligible to participate in subsequent layers, where they can be recomputed and cached when necessary. Consequently, SPTS improves dual-phase efficiency while enabling more flexible KV cache management, ensuring that informative tokens can be adaptively preserved across layers and thereby delivering improved accuracy.

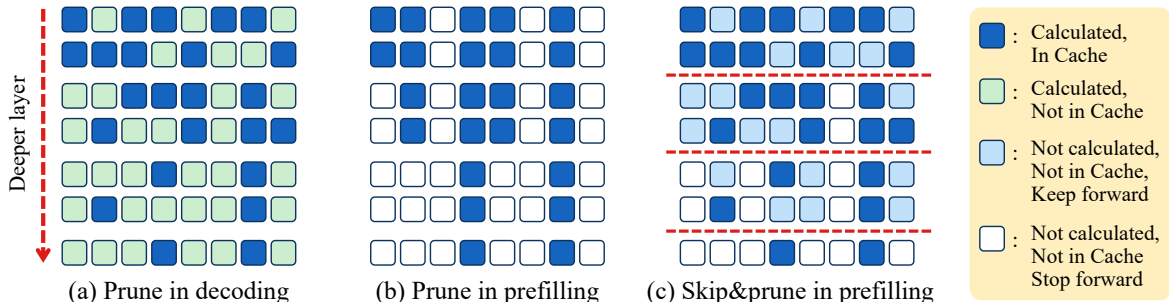


Figure 5. Illustration of different schemes in KV Cache management. (a) Decoding-phase pruning computes all tokens, offering no speedup in prefilling. (b) Prefilling-phase pruning discard tokens to reduce computation, but cached tokens exist only in the early consecutive layers, leading to noticeable information loss. (c) SPTS combines skipping with delayed pruning, allowing skipped tokens to be recomputed and cached later. It achieves the same computation costs as (b) while preserving richer contextual information.

## C. More Experimental Results and Analysis

**Ablation on Scale of the Low-rank Proxy Network** We investigate the effect of  $D_{\text{low}}$  and  $r$  in Sec. 3.3, which directly determine the scale of the proxy network used for token selection. Following previous experimental setup in Sec. 4.3, we only apply token skipping to FFN blocks. As shown in Tab. 6, increasing  $D_{\text{low}}$  and  $r$  enhances the fidelity of the proxy network in approximating the original FFN, which allows more accurate prediction of token-wise transformations. This, in turn, enables more precise selection of critical tokens, thus reducing the performance degradation caused by reduced feed-forward computation. However, larger values also increase the computational overhead associated with token selection, which we quantify in terms of FLOPs (Floating-Point operations) per token per projection.

Moreover, we also include settings that separately remove the  $D_{\text{low}}$  reduction and the  $r$ -based SVD decomposition, revealing that preserving the rank  $r$  is more critical to the effectiveness of the proxy network. In particular, the configuration  $(D_{\text{low}}, r) = (/, 192)$ , which exhibits a notable gap between the two dimensions of reduced projection matrix (*i.e.*  $U$  and  $V$ ), fails to adequately approximate the transformations of high-dimensional FFN layers, leading to substantially larger performance variations across datasets. These results suggest that, under a fixed selection budget, a more balanced low-rank design can help improve modeling fidelity.

Accordingly, to achieve a practical trade-off between selection efficiency and prediction accuracy, we empirically adopt a moderate  $(D_{\text{low}}, r)$  configuration.

**Effect of Utilizing Top Saliency Values** We evaluate the effect of utilizing top- $\rho$  fraction in Eq. (10). As reported in Tab. 7, retaining only the top values for dimension importance estimation consistently yields higher average accuracy. This design is motivated by the observation that intermediate activations in LLMs exhibit large variations (?). Therefore, intuitively, prioritizing the consistently highly activated dimensions preserves the most informative channels, enabling the proxy sub-network to better approximate the original FFN transformations and more accurately identify crucial tokens for reduced computation.

**Probe and Skip: Self-Predictive Token Skipping for Efficient Long-Context LLM Inference**

Table 6. Effect of  $D_{low}$  and  $r$  on per-token per-projection FLOPs and accuracy for LLaMA across five representative LongBench subsets. ‘/’ indicates that the corresponding dimension is not decomposed. The default setting is underlined.

$D_{low}$	$r$	FLOPs	Qasper	HPQA	TQA	LSHT	LCC
512	128	590K	43.67	53.60	91.17	45.00	57.49
512	256	1180K	44.00	54.36	92.04	45.50	57.76
512	/	2097K	43.85	55.18	92.03	46.00	58.36
<u>512</u>	<u>192</u>	855K	43.85	54.11	91.59	45.00	57.65
256	192	836K	43.17	53.38	91.33	45.50	57.55
1536	192	1081K	43.87	53.93	91.64	46.00	57.79
/	192	2900K	42.70	55.75	91.08	46.50	58.97

Table 7. Effect of selecting top- $\rho$  saliency values for channel importance on LLaMA. Results are reported on representative LongBench subsets and the average score (Avg.) on the full dataset. The default setting is underlined.

Method	MQA	HPQA	2WiKi	MuSiQue	QMSum	TREC	LSHT	Count	LCC	Avg. (%)
w/o top- $\rho$	54.64	52.68	45.71	30.24	24.65	72.00	46.00	6.21	63.19	47.56
<u>w/ top-<math>\rho</math></u>	<u>55.37</u>	<u>53.66</u>	<u>46.69</u>	<u>30.43</u>	<u>24.73</u>	<u>72.50</u>	<u>46.50</u>	<u>7.24</u>	<u>63.14</u>	<b>47.80</b>

**Ablation on Partial Attention Score** Given that several prior works estimate token importance using attention between input tokens and the last few tokens (Long et al., 2025; Xu et al., 2025), we conduct an ablation on the length of query tokens for probing partial attention in Eq. (4). As reported in Tab. 8, our default design, which relies solely the last token, achieves superior average performance. Intuitively, under our token skipping strategy, which is primarily applied in deeper layers, the last token already provides strong task generalization capability. In contrast, averaging attention signals over multiple tokens may introduce semantic ambiguity for certain complex tasks, leading to noticeable performance fluctuations, e.g., on Count and TREC. These results further suggest a potential direction for future work, where task-aware or adaptive probing strategies could be explored to better tailor token importance estimation to different task characteristics.

Table 8. Effect of query token length for PAP on LLaMA. Results are reported on representative LongBench subsets and the average score (Avg.) on the full dataset. The default setting is underlined.

Query Length	MQA	HPQA	2WiKi	MuSiQue	QMSum	TREC	LSHT	Count	LCC	Avg. (%)
64	54.33	52.67	43.95	31.31	24.29	63.00	45.00	7.38	63.32	47.00
4	54.53	54.83	45.39	30.58	25.23	70.50	46.50	4.77	62.85	47.53
<u>1</u>	<u>55.37</u>	<u>53.66</u>	<u>46.69</u>	<u>30.43</u>	<u>24.73</u>	<u>72.50</u>	<u>46.50</u>	<u>7.24</u>	<u>63.14</u>	<b>47.80</b>